

Woodpile-type photonic crystals with orthorhombic or tetragonal symmetry formed through phase mask techniques

Yuankun Lin, David Rivera

Department of Physics and Geology, University of Texas-Pan American, Edinburg, Texas 78541
linyk@panam.edu

K. P. Chen

Department of Electrical and Computer Engineering, University of Pittsburgh, Pittsburgh, PA 15261

Abstract: This paper simulates the photonic band structure in face-centered-orthorhombic and face-centered-tetragonal woodpile-type photonic crystals and shows the fabrication feasibility of these crystals with phase mask based holographic lithography. The experimental demonstration on SU-8 photoresist indicates that a single optical element can replace a complex optical setup for the holographic fabrication of woodpile-type photonic crystals. Photonic band gap calculation predicts the existence of full band gap in these crystals. Optimum band gap sizes are studied for crystals formed under various experimental conditions.

© 2006 Optical Society of American

OCIS codes: (999.9999) Photonic crystal; (220.4000) Microstructure fabrication; (260.3160) Interference; (220.0220) Optical design and fabrication; (090.0090) Holography.

References and links

1. J. D. Joannopoulos, P. R. Villeneuve, and S. H. Fan, "Photonics crystals: putting a new twist on light," *Nature (London)* **386**, 143-147 (1997).
2. V. Berger, O. Gauthier-Lafaye, and E. Costard, "Photonic band gaps and holography," *J. Appl. Phys.* **82**, 60-64 (1997).
3. M. Campbell, D. N. Sharp, M. T. Harrison, R. G. Denning, and A. J. Turberfield, "Fabrication of photonic crystals for the visible spectrum by holographic lithography," *Nature (London)* **404**, 53-56 (2000).
4. O. Toader, T. Y. M. Chan, and S. John, "Photonic band gap architectures for holographic lithography," *Phys. Rev. Lett.* **92**, 043905/1-4 (2004).
5. T. Y. M. Chan, O. Toader, and S. John, "Photonic band gap templating using optical interference lithography," *Phys. Rev. E* **71**, 046605/1-18 (2005).
6. D. N. Sharp, A. J. Turberfield, and R. G. Denning, "Holographic photonic crystals with diamond symmetry," *Phys. Rev. B* **68**, 205102-6 (2003).
7. N. D. Lai, W. P. Liang, J. H. Lin, C. C. Hsu, and C. H. Lin, "Fabrication of two- and three-dimensional periodic structures by multi-exposure of two-beam interference technique," *Opt. Express* **13**, 9605-9611 (2005), <http://www.opticsexpress.org/abstract.cfm?URI=OPEX-13-23-9605>.
8. S. Shoji, H. Sun, and S. Kawata, "Photofabrication of wood-pile three-dimensional photonic crystals using four-beam laser interference," *Appl. Phys. Lett.* **83**, 608-710 (2003).
9. I. Divliansky, T. S. Mayer, K. S. Holliday, and V. H. Crespi, "Fabrication of three-dimensional polymer photonic crystal structures using single diffraction element interference lithography," *Appl. Phys. Lett.* **82**, 1667-1669 (2003).
10. Y. Lin, P. R. Herman, and K. Darmawikarta, "Design and holographic fabrication of tetragonal and cubic photonic crystals with phase mask: toward the mass-production of three-dimensional photonic crystals," *Appl. Phys. Lett.* **86**, 071117/1-3 (2005).
11. Cheng Lu, X. K. Hu, I. V. Mitchell, and R. H. Lipson, "Diffraction element assisted lithography: Pattern control for photonic crystal fabrication," *Appl. Phys. Lett.* **86**, 193110/1-3 (2005).
12. Y. Lin, P. R. Herman, and E. L. Abolghasemi, "Proposed single-exposure holographic fabrication of microsphere-type photonic crystal through phase mask techniques," *J. Appl. Phys.* **97**, 096102/1-3 (2005).
13. M. J. Escuti, J. Qi, and G. P. Crawford, "Tunable face-centered-cubic photonic crystal formed in holographic polymer dispersed liquid crystals," *Opt. Lett.* **28** (7), 522-524 (2003).

14. Y. K. Pang, J. C. Wai Lee, H. F. Lee, W. Y. Tam, C. T. Chan, and P. Sheng, "Chiral microstructures (spirals) fabrication by holographic lithography," *Opt. Express* **13**, 7615-7620 (2005), <http://www.opticsexpress.org/abstract.cfm?URI=OPEX-13-19-7615>.
15. H. Miguez, N. Tetreault, B. Hatton, S. M. Yang, D. Perovic, G. A. Ozin, "Mechanical stability enhancement by pore size and connectivity control in colloidal crystals by layer-by-layer growth of oxide," *Chem. Commun. (Cambridge)* **22**, 2736-2737 (2002).
16. N. Tetreault, G. von Freymann, M. Deubel, M. Hermatschweiler, F. Perez-Willard, S. John, M. Wegener, and G. A. Ozin, "New route to three-dimensional photonic bandgap materials: silicon double inversion of polymer templates," *Adv. Mater.* in press (2005).
17. S. G. Johnson and J. D. Joannopoulos, "Block-iterative frequency-domain methods for Maxwell's equations in a planewave basis," *Opt. Express* **8**, 173-190 (2001), <http://www.opticsexpress.org/abstract.cfm?URI=OPEX-8-3-173>.

1. Introduction

A photonic crystal is a dielectric medium in which periodic microstructures are formed using high refractive index contrast materials. Since its first introduction in 1987, a large number of applications have been proposed using photonic crystal structures [1]. However, it has been a great challenge to rapidly fabricate large-area and defect-free three-dimensional (3D) photonic crystals at low cost. Holographic lithography has recently been employed to fabricate 3D photonic crystals by exposing a photoresist or polymerizable resin to interference patterns of laser beams [2-14]. This multi-beam interference technique has produced defect free, nanometer-scale structures over large substrate areas [3]. Photonic structures are defined in photoresist by iso-intensity (iso-laser dosage) surfaces of interference patterns [4, 5]. A desired geometrical structure could be obtained by single or multiple exposures [6-8, 10]. The holographic lithography has also been used to produce tunable photonic crystals in a liquid crystal and polymer system [13], and to demonstrate a chiral microstructure in SU-8 photoresist [14]. In the case of positive resist, the overexposed material is then dissolved away in the post-exposure processing. The underexposed region forms a periodic network and acts as a 3D photonic crystal template. The template can then be infiltrated at room temperature with SiO₂ and burned away, leaving behind a daughter "inverse" template [15, 16]. Finally, the daughter template is inverted by infiltration with silicon and selective etching of the SiO₂ [16].

However, fabrication strategies that rely on interference of multiple independent beams can introduce alignment complexity and inaccuracies due to differences in the optical path length and angles among the interfering beams as well as vibrational instabilities in the optical setup [9]. In order to improve the optical setup, diffractive optics elements or phase masks have been introduced to create the interference pattern for the holographic fabrication of photonic crystals [9-12]. When a single beam goes through a diffractive optics element or a phase mask, an interference pattern will be formed behind these optical devices [10-12]. If designed properly, a single optical element can replace a complex optical setup to generate a desired interference pattern. Another advantage of these single optical element techniques is that they are compatible with the conventional photolithography so that people can take advantage of standard tools of the electronics industry for the fabrication of 3D photonic crystals. The phase mask technique, which can use laser power much efficiently, will be an industry-favored approach for the holographic fabrication of 3D photonic crystal.

In this paper we studied the interference pattern formed through the phase mask. For the first time to our best knowledge, we demonstrated that a series of woodpile-type photonic crystal templates with tetragonal or orthorhombic symmetries can be practically fabricated in a photoresist if exposed to the interference pattern generated through the phase mask. Detailed photonic band gap calculations have revealed the existence of a photonic full band gap in these structures if the photonic crystal template is converted into silicon.

2. Theoretic description

As shown in Fig. 1 (left), when a single beam goes through a one-dimensional phase mask, the beam will be diffracted into three beams. Beams 1 and 2 are from first order diffraction

and beam 3 is from zero order diffraction. Beam 1 or 2 has a diffraction angle θ relative to beam 3. Mathematically these three beams are described by:

$$\vec{E}_1(\vec{r}, t) = E_1 \cos((k \cos \theta) z - (k \sin \theta) x - \omega t + \delta_1), \quad (1)$$

$$\vec{E}_2(\vec{r}, t) = E_2 \cos((k \cos \theta) z + (k \sin \theta) x - \omega t + \delta_2), \quad (2)$$

$$\vec{E}_3(\vec{r}, t) = E_3 \cos(k z - \omega t + \delta_3). \quad (3)$$

k and ω are the wave vector and angular frequency of the beam, respectively, E is the constant of electric field strength, and δ is the phase of the beam. These three beams will generate a two-dimensional interference pattern. The interference pattern is determined by the laser intensity distribution I in 3D space:

$$\begin{aligned} I = & \frac{1}{2} E_1^2 + \frac{1}{2} E_2^2 + \frac{1}{2} E_3^2 + (E_1 \cdot E_2) \cos((2k \sin \theta)x + (\delta_2 - \delta_1)) \\ & + (E_1 \cdot E_3) \cos((2k \sin^2(\frac{\theta}{2}))z + (k \sin \theta)x + (\delta_3 - \delta_1)) \\ & + (E_2 \cdot E_3) \cos((2k \sin^2(\frac{\theta}{2}))z - (k \sin \theta)x + (\delta_3 - \delta_2)) \end{aligned} \quad (4)$$

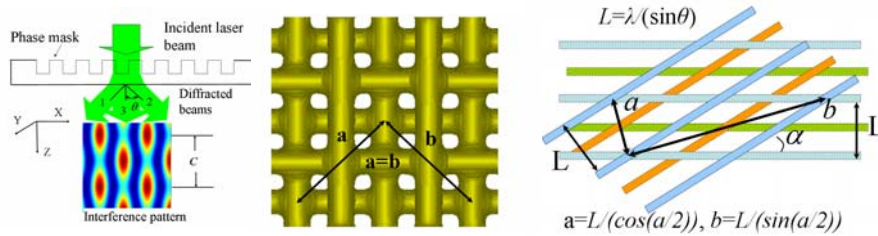


Fig. 1. (left) phase mask based interference. A phase mask can replace a complex optical setup for a generation of interference pattern; (middle) a simulated woodpile-type photonic structure formed in the doubly-exposed photoresist; (right) a schematic illustration of woodpile-type photonic structure with orthorhombic or tetragonal symmetry and its lattice constants.

As shown in Fig. 1 (left), these three beams are overlapped if the beam size is big enough. Fig. 1 (left) shows the interference pattern generated behind the phase mask, assuming the incident laser beam has a polarization in y direction. The interference pattern is periodic in the z -direction as well as in x -direction. The periodicity of the interference pattern along x direction is $\lambda/(\sin\theta)$ (where λ is the wavelength of laser beam generating the interference pattern). The periodicity c of the interference pattern along z direction is $\lambda/(2\sin^2(\theta/2))$. After the photoresist is exposed to such interference pattern, the sample is rotated by an angle of α along the propagation axis of the incident beam and its position is displaced along the laser propagation direction by $1/4$ times $\lambda/(2\sin^2(\theta/2))$. The distance of moving the sample is about submicron. It can be achieved through a motor driven linear motion stage with a resolution of 50 nm. The rotation can also be controlled by a motor driven rotation stage with a wobble of 70 μ rad so that the sample is kept almost unmoved in the z direction during the rotation process. Then the photoresist receives second exposure. The doubly-exposed photoresist is then developed to form a 3D woodpile-type photonic crystal template. Fig. 1 (middle) shows a simulated photonic structure formed with the rotation angle $\alpha=90$ degree if a negative photoresist is used. After the photoresist development, the under-exposed area is dissolved away while the area exposed with above-threshold laser dosage is networked to form periodic structures. We illustrate in Fig. 1 (right) how we construct crystal lattices. We set a fundamental length scale $L=\lambda/(\sin\theta)$ for such structure because the three beam interference pattern is determined by the laser wavelength and the interference angle θ . L is actually equal to the grating period of the phase mask. The lattice constants in xy plane depend on the angle α . They are related by $a=L/(\cos(\alpha/2))$ and $b=L/(\sin(\alpha/2))$, respectively. The photonic crystal template has a lattice constant along the z direction $c= \lambda/(2\sin^2(\theta/2))=L(\cot(\theta/2))$. If the

sample rotation angle α is 90 degree, we have $a=b$. Thus the 3D structure has a face-centered-tetragonal or face-centered-cubic symmetry [10]. If the angle α is less than 90 degree, a face-centered-orthorhombic ($a \neq b \neq c$) or face-centered-tetragonal ($a \neq b = c$) structure is formed in the photoresist.

3. Photonic band gap calculation

The woodpile-type photonic crystal template will be converted into high refractive index materials using the approach of CVD infiltration [15, 16] in order to achieve a full band gap photonic crystal. We calculated the photonic band gap for converted silicon structures where “woods” are in air while the background is silicon. The calculation has been performed for photonic structures formed with various interference angles θ and rotation angles α . Fig. 2 (left) shows the first Brillouin surface of the face-centered-orthorhombic lattice. Coordinates of high symmetric points on the Brillouin surface varies with different structures. MIT Photonic-Bands Package [17] was used to calculate the photonic band gap of the converted silicon structure. Fig. 2 (right) shows the photonic band structure for the converted silicon woodpile-type structure with $c/L=2.4$ and $\alpha=51$ degree (the dielectric constant of 11.9 was used for silicon in the calculation [4, 5]). We would like to clarify that the λ_{photon} in the y-axis label of the Fig. 2 (right) is the wavelength of photons in the photonic band, not the wavelength of the exposure laser. The band structure shows that a photonic full band gap exists between the 2nd and 3rd bands with a band gap size of 8.7 % of the gap center frequency.

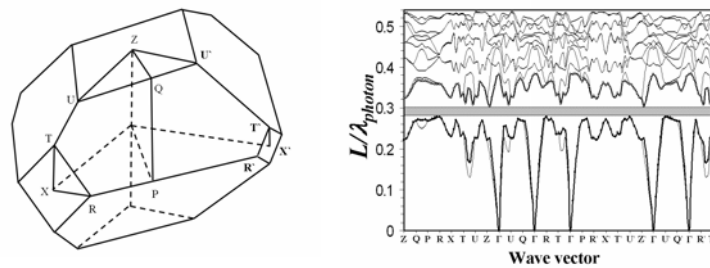


Fig. 2. (left) First Brillouin surface of face-centered-orthorhombic lattice; (right) photonic band structure for an orthorhombic photonic crystal. λ_{photon} is the wavelength of photons in the photonic band

Figure 3 (left) shows optimum photonic band gap sizes as a function of rotation angle α for photonic crystal structures formed at different interference angles θ . When the rotation angle α is less than 90 degree, the band gap size initially decreases with the reduced angle α . With further decreasing rotation angle α , the band gap size starts to increase. After reaching a maximum value, the band gap size decreases again with reduced rotation angles. The variation of band gap size is closely related to the change of symmetry of photonic crystal structures. Given the lattice constants (a, b, c) are ($L/(\cos(\alpha/2)), L/(\sin(\alpha/2)), L(\cot(\theta/2))$) respectively, the fabrication process with the rotation angle $\alpha=90$ degree produces a tetragonal symmetry for the photonic crystal structure with the lattice constant $a=b$. With decreasing angle α , photonic crystals with an orthorhombic symmetry is formed with $a \neq b \neq c$. The bandgap starts to increase with the decreasing rotation angle α when the rotation angle α is approaching to a point such that $1/\sin(\alpha/2) = \cot(\theta/2)$ where a structure with tetragonal symmetry is formed with lattice constants $b=c$. Further decreasing of the rotation angle reverses the trend of bandgap size as a function of rotation angle α . For the photonic crystal structure formed at a larger interference angle θ , the rotation angle has a value close to 90 degree in order to have a tetragonal symmetry with $b=c$. The maximum band gap size is reached when $b=c$. However the rotation angle is smaller in order to have the tetragonal symmetry with $b=c$ in structures

formed at a smaller interference angle θ . Second exposure after a smaller rotation angle produces a photonic crystal microstructure not ideal for an optimum of photonic band gap size although $b=c$. Instead the maximum band gap occurs in a structure where b is slightly less than c . For the case of $c/L=2.3$, the rotation angle $\alpha=51.5$ degree is needed in order to have $b=c$ thus a tetragonal structure. As seen from Fig. 3 (left), an optimum band gap occurs in the structure where the rotation angle $\alpha=55$ degree.

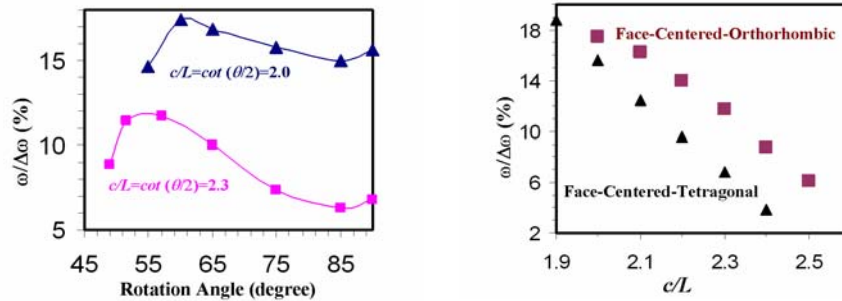


Fig. 3. (left) Photonic band gap size as a function of rotation angles for photonic crystal with $c/L=2.3$ and $c/L=2.0$. (right) photonic band gap size in face-centered-tetragonal structures ($\alpha=90$ degree) and in face-centered-orthorhombic structures (α less than 90 degree) for various structures with a different c/L value.

Figure 3 (right) shows the optimum band gap size in face-centered-tetragonal photonic structures which is formed with the rotation angle $\alpha=90$ degree and in face-centered-orthorhombic structure where $\alpha \neq 90$ degree, under different beam interference geometries. When c/L is small (beams have a larger interference angle), a rotation angle of 90 degree is preferred in order to have a larger band gap. However if c/L is larger than 2.0, then the face-centered-orthorhombic structure is preferred for a larger band gap. At $c/L=2.3$, the optimum band gap size is 11.7% of the gap-center frequency for a face-centered-orthorhombic structure formed with a rotation angle near 55 degree. While the face-centered-tetragonal structure formed with $\alpha=90$ degree has a gap size of 6.7%.

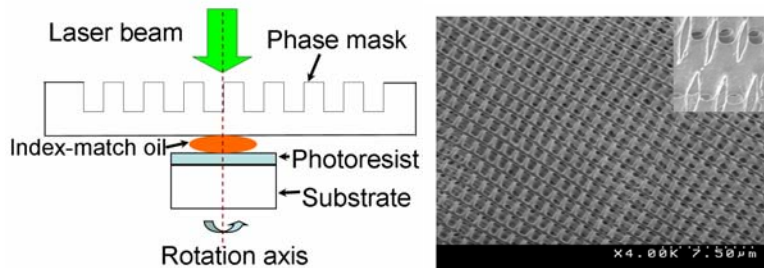


Fig. 4. (left) an arrangement of the phase mask and the photoresist. The interface between the backside of the phase mask and the photoresist is wetted with an index-match fluid; (right) SEM top-view of a woodpile-type structure in SU-8TM photoresist formed through the phase mask based holographic lithography. The insert is a side-view of the SU-8 structure.

4. A proof-of-principle demonstration

Utilizing the phase mask method a number of photonic structures can be generated; however there are some practical issues in realizing a photonic structure with a photonic full band gap. Fig. 3 (right) shows that a photonic band gap exists in structures with smaller c/L values.

Because $c/L=\cot(\theta/2)$, a bigger interference angle is required in order to generate an interference pattern for a structure with a photonic full band gap. When the photoresist is exposed to an interference pattern, the interference pattern inside the photoresist will be different from that in air. In the case of $c/L=\cot(\theta/2)=2.5$, an interference angle $\theta=43.6$ degree is required, which is greater than the critical angle of most of photoresist. In order to expose the photoresist to an interference pattern formed under a bigger interference angle, a special setup is arranged for the phase mask and the photoresist as shown in Fig. 4 (left). The photoresist is placed on the backside of the phase mask with the contact surface wetted with an index-match mineral oil. The design of the phase mask is modified correspondently. As a proof-of-principle, we have fabricated photonic crystals with rotation angles of 90, 60 and 45 degrees through the phase mask based holographic lithography. 514 nm line from an Ar ion laser was used for the exposure of 10 μm thick SU-8TM photoresist spin-coated on the glass slide substrate. The SU-8 photoresist was modified by adding H-Nu 470 and OPPI photo-initiators (Spectra Group Limited) to make the photoresist sensitive to 514 nm. The photoresist and phase mask were both mounted on high-precision Newport stages. Both the phase mask and photoresist were kept perpendicular to the propagation axis of the incident Ar laser beam as shown in Fig. 4 (left). The modified photoresist was exposed to the laser beam with a power of 1 W and a size of 1 mm for 4 seconds. We show in Fig. 4 (right) SEM of fabricated structures in SU-8TM photoresist with the rotation angle $\alpha=90$ degree. The side-view of the SU-8 structure is shown in the insert of the Fig. 4 (right). The top-view of the SEM shows layer-by-layer structures, in agreement with the simulated structure in Fig. 1 (middle). The side-view of the structure demonstrates the typical interference pattern as shown in Fig. 1 (left). The fabricated SU-8 structure is indeed a woodpile-type photonic crystal template. The detail fabrication results will be reported elsewhere.

5. Summary

In summary, we have demonstrated for the first time to our best knowledge that both face-centered-orthorhombic and face-centered-tetragonal woodpile-type photonic crystals can be fabricated through phase mask based holographic lithography. The phase mask approach has simplified the optical setup for the holographic fabrication of 3D photonic crystals. The woodpile-type structure and band gap of photonic crystal can be controlled by the holographic lithography. Our simulation predicts that a full band gap exists in both orthorhombic and tetragonal structures. The study not only leads toward a possibility of fabrication of photonic crystals through holographic lithography for structures beyond intensively-studied cubic symmetry but also provides a blueprint defining the lattice parameter for an optimum band gap in these orthorhombic or tetragonal structures.